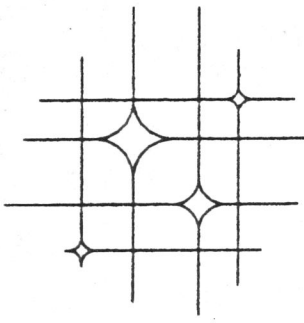

ASTRONET SPECIAL PUBLICATION 88/1

Super-Computing in Astrophysics

Proceedings of a Workshop held at
Osservatorio Astronomico di Roma
Monteporzio Catone, 10–11 March 1988

Edited by F. Vagnetti

Comitato di Gestione ASTRONET
CNR – Gruppo Nazionale di Astronomia
Osservatorio Astronomico di Roma
Dipartimento di Fisica – II Università di Roma

DYNAMICAL EVOLUTION OF TYPE II SUPERNOVAE. INTERACTION WITH A PRE-EXISTING BUBBLE

L. Ciotti, R. Bedogni, A. D'Ercole

Osservatorio Astronomico, Bologna

I. Introduction

It is well known that Type II Supernovae explosion originates at the end of the life of massive stars. The mass range of the progenitors is not firmly established, but it is belived to be above $8M_{\odot}$. Such stars spend the largest part of their life on the main sequence ($t_{ms} = 0.9t_{tot}$); during this time ($10^7 yr$ for a $15M_{\odot}$ star) they loose a substantial fraction of their mass through the stellar wind mechanism with velocities V_w of about $2000\, kms^{-1}$ and mass loss rates $\dot{M}$ of about $10^{-6} \div 10^{-7} M_{\odot} yr^{-1}$.

It has been shown that the interaction of such a fast wind with the surrounding interstellar medium generates a large cavity, or "*bubble*". The interior of the bubble is filled with hot ($T > 10^6 K$) shocked stellar wind at low density and the swept-up interstellar gas is compressed into a thin, spherical shell (Weaver et al., 1977).

When the star becomes a red supergiant ($t_{rg} = 0.1t_{tot}$), the mass loss properties change. The mass loss rate $\dot{M}$ becomes of the order of $10^{-5} M_{\odot} yr^{-1}$, while the stellar wind velocity becomes as low as $20\, kms^{-1}$. It is quite natural therefore to assume that, when the SN explosion occours, stellar ejecta expands into a medium with a r^{-2} density profile, provided that $\dot{M}$ and V_w remain constant.

On the other hand numerical models show that stellar material ejected by the supernova explosion moves in free expansion with the velocity linearly increasing with radius and the density decreasing as r^{-n}. The interaction of this stellar material with the circumstellar medium consisting of the previous red supergiant slow wind gives rise to an interaction region which contains shocked ambient gas as well as shocked stellar ejecta. This region tends toward the self-similar solution given by Chevalier (1982). Such a solution holds as long as the unperturbed density distribution of both the ejecta and the circumstellar medium mantains the power low radial dependence. Howewer the external shock will eventually reach the pre-existing bubble and the problem will be no longer self-similar.

Numerical computations are therefore needed to describe the later evolution of the supernova remnant (SNR).

II. Supernovae

The interaction region described by the Chevalier solution consists of two

parts: the outer shell composed of the swept-up circumstellar material and the inner one containing the shocked stellar ejecta. These two shells are separated by a contact discontinuity. At this discontinuity the density of both shocked stellar and circumstellar material tends to approach infinity while the temperature tends towards zero (see fig. 1).

III. Bubble

We compute the bubble structure (that will interact whit the SNR) following the idealized interstellar bubble theory of Weaver et al. (1977). The assumptions of the idealized model are:

(1) the ambient interstellar medium has uniform constant density $\rho_o = \mu m_H n_o$
(2) the star is at rest with respect to the interstellar medium,
(3) the stellar wind is isotropic,
(4) the wind power $L_w = \dot{M} V_w^2/2$ is constant.

These assumptions are of course oversimplified. In particular, the uniformity of the interstellar medium may be questionable. McKee et al. (1984) investigated how the evolution of a stellar wind bubble modifies in a cloudy ambient medium.

During the main sequence lifetime, t_{ms}, photo-evaporation by the Lyman radiation will tend to homogenize an initially cloudy medium of mean density n_m out to a radius

$$R_h(t_{ms}) = 56 n_m^{-0.3} pc \qquad (1)$$

The stellar wind will sweep a dense shell from the homogenized region and will leave a low density bubble around the star.

When the homogenization radius is reached, further expansion will be primarily constrained by the rate of growth of the homogenization radius. As long as the bubble expands the pressure of the hot gas decreases and eventually reaches the value of the pressure of the external HII region at a temperature $T_{HII} = 8000K$. At this time the exterior pressure becomes crucial and causes the outer shell to stall.

After that the bubble becomes stationary as long as $\dot{M}$ and V_w remain constant. It can be shown that the radius of the bubble is smaller than R_h (Weaver et al., 1977). This means that even if the bubble tends to overrun the radius of homogenization R_h during its dynamical phase engoulfing a number of clouds, later on R_h tends still to grow while R_{Bubble} remains at rest. In other words the bubble is eventually surrounded by homogeneus medium.

We are interested only in the stationary structure of the bubble rather then in its evolution and we therefore make the same simplifing assumption of Weaver et al. (1977) in computing the bubble evolution (see fig.2).

IV. Numerical code

We computed the expanding bubble and its interaction with the SNR in two separated steps. First we followed the bubble making use of a moving grid which follows the interacting region; in this way we mantain a quite high relative spatial resolution at any time during the expansion. In the second step we calculated the expansion of the supernova adopting the Chevalier solution as initial conditions. Also in this case we use a moving grid.

The linear dimensions of the stationary bubble are of course much greater than that of the SNR in the beginning of the interaction. We were therefore forced to adopt, in computing the bubble, a grid with a huge number of zones (800), in order to get a spatial resolution comparable with that of the supernova calculation (with a grid of 200 mesh points).

IV.1 The remapping

During the computation of the expanding SNR the presence of the bubble is considered through the boundary conditions at the external edge of the grid. In other words, as long as the SNR merges in the bubble, the hydrodinamical variables in the last mesh must be obtained taking in account the values of the variables of the bubble at that point. The numerical meshes of the supernova being smaller than that of the bubble, the evaluation of the external boundary conditions are obtained through a "*remapping*" of the bubble's variables over the last grid of the SNR. Such a remapping is performed following van Leer (1979).

IV.2 The code

We express the gasdynamics equations in Eulerian form with spherical symmetry. To integrate these equations we make use of scheme II of van Leer (1977). It is an *upwind* scheme in which the variables are approximated by linear functions inside each mesh.

The SLIC algoritm (Noh and Woodward, 1977) allows to follow exactly the contact surface.

Consider now the equation of continuity:

$$\frac{\partial \rho}{\partial t} + div(\rho v) = 0 \tag{2}$$

the equation of motion:

$$\frac{\partial \rho v}{\partial t} + div(\rho v^2) = -\frac{\partial p}{\partial r} \tag{3}$$

and the equation of energy:

$$\frac{\partial E}{\partial t} + div(Ev) = -p\, div(v) - div(q) - L \tag{4}$$

where q is the *heat flux* due to thermal conduction (Spitzer, 1962):

$$q = -k(T)\frac{\partial T}{\partial r} \tag{5}$$

k is the *conduction coefficient* and L is the *radiative luminosity*. The two most time-consuming routines in our code are those solving the divergence operator and the heat diffusion term. This last term is isolated making use the time splitting method (Richtmyer and Morton, 1967) and integrated separately following the Crank-Nicholson method. This leads to the following numerical algorithm for the interior points:

$$-A_J T_{J+1} + B_J T_J - C_J T_{J-1} = D_J \tag{6}$$

where A_J, B_J, C_J are coefficients which contains, among others, the conduction coefficient k, while D_J is the known term. The solution is given by:

$$T_{J-1} = G_{J-1} T_J + H_{J-1} \tag{7}$$

where:

$$G_J = \frac{A_J}{B_J - C_J G_{J-1}} \tag{8}$$

$$H_J = \frac{D_J + C_J H_{J-1}}{B_J - C_J G_{J-1}} \tag{9}$$

The left-hand boundary condition will determine G_1 and H_1, after which the recursive relations (8) e (9) can be used to calculate all G and H up to $J = J_{max} - 1$. Then T_{jmax} is set from the right-hand boundary condition, and equation (7) is used with the known A, B, C, D, and calculated G and H to solve recursively for T_J from T_{J+1}, marching down from $J = J_{max} - 1$ to $J = 1$. Because of the longer characteristic time-scale diffusion process in front of the dynamical time-scale, many iterations are needed at each time-step before to reach a sufficient convergence ($|T^{i+1} - T^i|/T^i < 10^{-4}$). Unfortunately, however, because of the recursive nature of such an algorithm, it can not be speeded by vectorisation.

On the other hand a considerable fraction of CPU time can be saved vectorising the routine that performs divergences.

As stated before we make use of the upwind finite difference scheme which possesses the desirable *transportive property*. The effect of a disturbance is advected only in the direction of velocity. This property is as physically significant as the conservative one. Schemes with space centered first derivatives are more accurate in the sense of truncation error. However a perturbation can travel in both directions, and the transportive property is lost. The algorithm for divergence (in slab geometry for the sake of simplicity) can be written in the following way:

$$\rho_J(t + \Delta t) - \rho_J(t) = -\frac{\Delta t}{\Delta R}(F_{J+1} - F_J) \tag{10}$$

were Δt is the time-step and $\Delta R = R_{J+1} - R_J$ is the size of the spatial mesh. The computation of the flux F at the boundary of the mesh depends on the sign of the fluid velocity v at that point.

$$if\ v > 0 \qquad F_J^l = v(\rho_{J-1/2} + .5(1-\sigma)S_{J-1/2})$$

$$if\ v < 0 \qquad F_J^r = v(\rho_{J+1/2} - .5(1+\sigma)S_{J+1/2})$$

where $\sigma = v\Delta t/\Delta R$ and $S_{J+1/2}$ is the slope of the linear function approximating ρ inside the mesh $(R_J; R_{J+1})$.
We do not give here the details to obtain the previous formulae (Bedogni and D'Ercole, 1986, see however fig.3). We just want to point out that the usual statement IF in a DO LOOP in order to check the sign of v at each boundary mesh is quite time expensive. Here however it is possible to get vectorisation making use of the CVMGP statement which works as follows: CVMGP(F_J^l, F_J^r, v_J). Such a statement selects F_J^l or F_J^r in a totally vectorised way depending on the sign of v_J.

In this way we obtain a gain of a factor of 10 in the computation of the divergence and a factor 2 in the run of the whole program.
For comparison we give the time spent for one cycle by the code which compute the bubble over a grid of 800 meshes:

$$VAX11/780 \qquad 8.05\ sec$$

$$CRAY - XMP\ (Non\ vectorised) \qquad 0.056\ sec$$

$$CRAY - XMP\ (Vectorised) \qquad 0.028\ sec$$

Acknowledgements. This work has been supported by M.P.I. 60%.

References

Bedogni, R., D'Ercole, A.:1986, *Astron. Astrophys.*, **157**, 101
Chevalier, R. A.: 1982, *Astrophys. J.* **258**, 790
McKee, C. F., Van Buren, D., Lazareff, B.: 1984, *Astrophys. J.* **278**, L115
Noh, W.F., Woodward, P.R.: 1977, in *Lecture Notes in Physics* No. 59, Springer-Verlag, Berlin
Richtmyer, R.D., Morton, K.W.: 1967, *Difference Methods for Initial-Value Problems*, Interscience, New York
Spitzer, L., Jr.: 1962, *Physics of Fully Ionized Gases*, Interscience, New York
van Leer, B.: 1977, *J. Computational Physics* **23**, 276
van Leer, B.: 1979, *J. Computational Physics* **32**, 101
Weaver, R., McCray, R., Castor, J.: 1977, *Astrophys. J.* **218**, 377

TABLE OF FIGURES

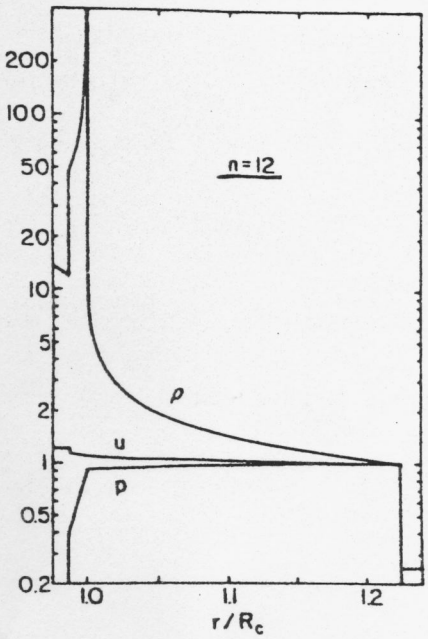

fig.1

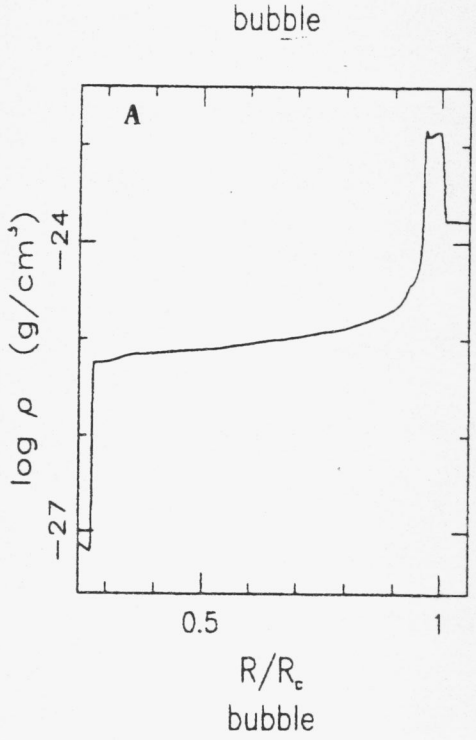

bubble

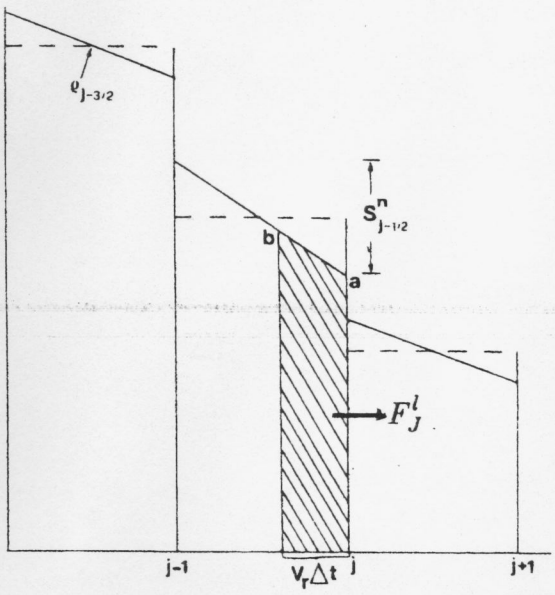

fig.3

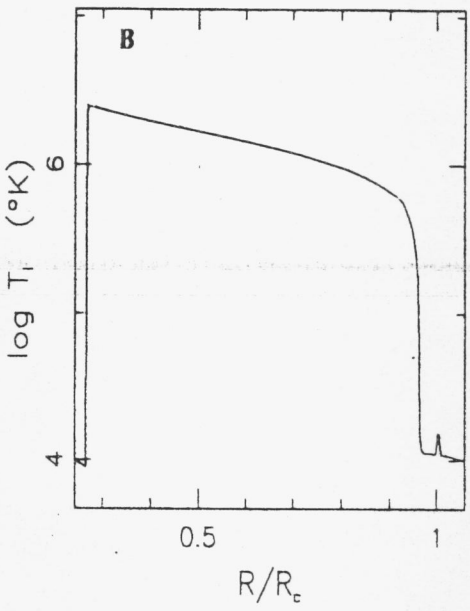

fig.2

fig.1 Chevalier solution (adapted from Chevalier, 1982)
fig.2 Density and temperature profile of the bubble
fig.3 Advection in slab geometry (Bedogni, R., D'Ercole, A.: 1986)